Transmission loss adaption of sandwich panels with honeycomb core variation

Martin Radestock[a]
Thomas Haase[b]
Hans Peter Monner[c]
German Aerospace Center
Institute of composite structures and adaptive systems
Lilienthalplatz 7
38122 Braunschweig, Germany

ABSTRACT

Nowadays the structures of an aircraft are stiff and lightweight. One example is the utilization of honeycomb sandwich panels, which are used in cabin linings or nacelles. From an acoustic point of view is such panel a disadvantage, because of the hollow core and the high stiffness to weight ratio. Acoustic waves can easily transmit through the structure, because only the thin face sheets prevent the sound transmission. However the honeycomb core influences the stiffness of the face sheets, because it is glued to them and as a result the core geometry has an influence to the sound transmission. That's why a design tool will be presented, which calculates a honeycomb core with a variable geometry and also regard a constant mass. The constant mass shall prevent a transmission loss improvement by adding additional mass. After the geometrical design, the tool calculates a transmission loss out of a finite element analysis. The results of the core variation show an interesting influence to the sound transmission. To realize these variable honeycomb cores an additive manufacturing is used for future research. The material for this honeycomb will be plastic and therefore the selected face sheets are out of glass fiber.

---

[a] email: Martin.Radestock@dlr.de
[b] email: Thomas.Haase@dlr.de
[c] email: Hans.Monner@dlr.de

1   INTRODUCTION

In the aircraft design, the minimization of the overall mass is essential, because it reduces directly the jet fuel. Nowadays the improvement is done with optimizers, where the main objectives are the stiffness and the mass. One example of stiff and lightweight structures is the honeycomb sandwich. The hollow core and the thin face sheets realize a high stiffness to weight ratio, but it also reduces the transmission loss (TL) of the structure[1]. The work of Kumar shows that different honeycomb core geometries have an influence on the loss factor[2]. Only a few honeycomb cores are analyzed in the work of Kumar. In order to analyze the geometrical parameters of honeycomb cores in detail a design tool is necessary to increase the number of different honeycomb cores.

Therefore, a honeycomb sandwich design tool is developed and TL simulations with varying geometry parameters are conducted. The paper is structured as follows: The first part describes the geometrical adaption with respect to a constant mass. If the core geometry is varied without an adaption of the wall thickness, the mass changes and subsequently also the TL. The second part of this paper describes the calculation of the TL with a planar wave excitation and the vibration of the radiating face sheet. The simulation model uses only the honeycomb sandwich as volume without any fluid elements. The last part shows results from single parameter variations and their effect on the TL.

2   SIMULATION MODEL

The flow chart in figure 1 explains the whole framework for the simulation in general with the single steps and the dependencies of the steps. The circles are the input data of the simulation, which can be varied for subsequent sensitivity analysis.

The geometrical parameters describe a complete honeycomb core in a 2D plane, which is the x-y plane in the model. After the core geometry is designed in the 2D plane the core is extruded as 3D model and the face sheets are added. The face sheets are out of glass fiber reinforced plastic. In the simulation the face sheets are not varied in material, thickness or dimensions. Furthermore, the honeycomb core is not varied in thickness direction and it is only extruded in z-direction. The geometrical model is generated in the software CATIA^{TM} as part design. Afterwards, the volume model is meshed in Ansys® Workbench^{TM}. The nodal coordinates of the mesh from one face sheet are transferred to the excitation generator. The generator calculates equivalent nodal forces, which minimizes computational costs, because fluid elements are not necessary. Equivalent means, that the nodal forces represents a pressure distribution above the face sheets, e.g. a diffuse sound field for TL simulations. With all boundary conditions the structural response is calculated and the displacement at the radiating surface is exported. The last step is the calculation of the sound transmission with the ratio of sound power on the excitation surface and the sound power on the radiating surface. The sound power of the excitation surface is estimated with the calculated pressure from the excitation generator. The sound power of the radiating surface is estimated with the Radiation Resistance matrix and the surface velocities. Hence, the complete model uses a three dimensional model without fluid elements in order to reduce the computational time.
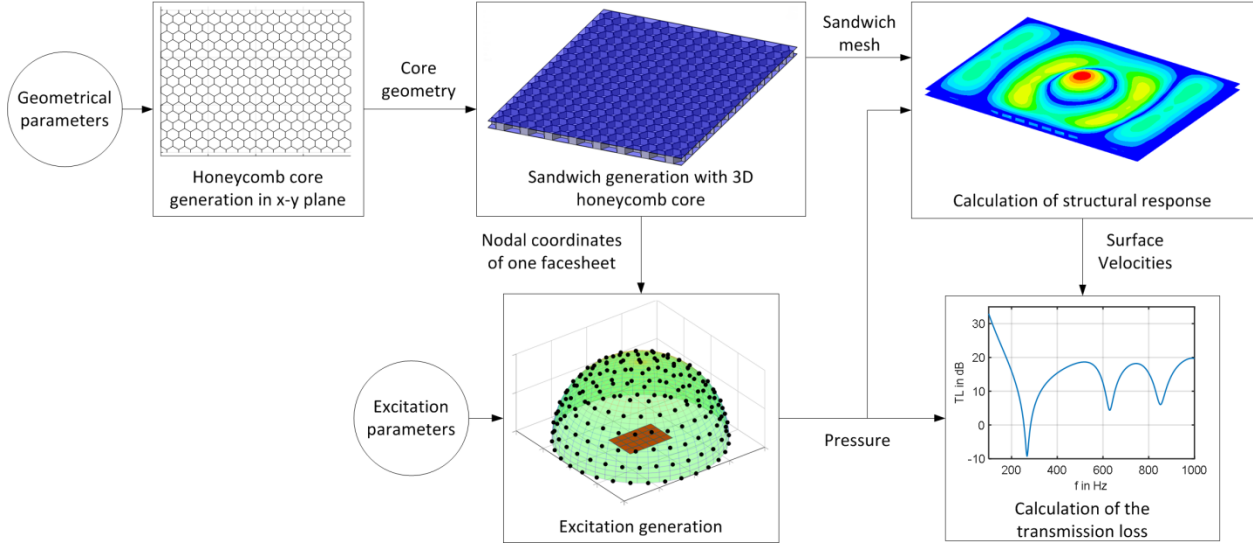
Fig. 1 – Flow chart of the simulation model for variable honeycomb cores.

2.1 Design of honeycomb core

The geometry of the honeycomb core is completely defined with 8 parameters. These parameters are the overall dimensions of the sandwich plate with length L_{PL}, width B_{PL} and height H_{PL}, the number of cells in vertical n_v and horizontal n_h direction, the cell angle α, the desired mass m_{tar} and the density of the core material ρ_{core}. The overall dimensions of the sandwich panel are fixed in this simulation. The length L_{PL} is 800 m, the width B_{PL} is 600 m and the height H_{PL} is 20 mm. The dimensions result from an existing experimental setup, which will be used for future experimental investigations.

Figure 2 shows the dimensions of the sandwich in the x-y plane with the length and the width. An arbitrary division is shown with dashed lines, which represents the number of cells in vertical and horizontal direction. Furthermore, a single honeycomb cell is shown in figure 2 and the dimensions of the cell are assigned. It has to be noticed that there are two different cell length l_{ver} and l_{dia}, because the cell angle α is a variable.

One assumption is that the thickness d of the honeycomb core walls is constant. The thread of the calculation is similar to literature[3]. The generated honeycomb core in literature is a beam model, while here a volume is generated, where the thickness d is relevant for the design. All solid lines of the honeycomb cell in figure 2 present the middle line for extension in the plane. From this middle line the thickness d is extended in both directions as it is indicated in figure 2 with a dotted line. Especially at the borders of the plate, the honeycomb core is then sticking out by d/2. Therefore, the cell lengths are calculated with the following equations.

$$l_x = \frac{L_{PL} - d}{n_h} \tag{1}$$

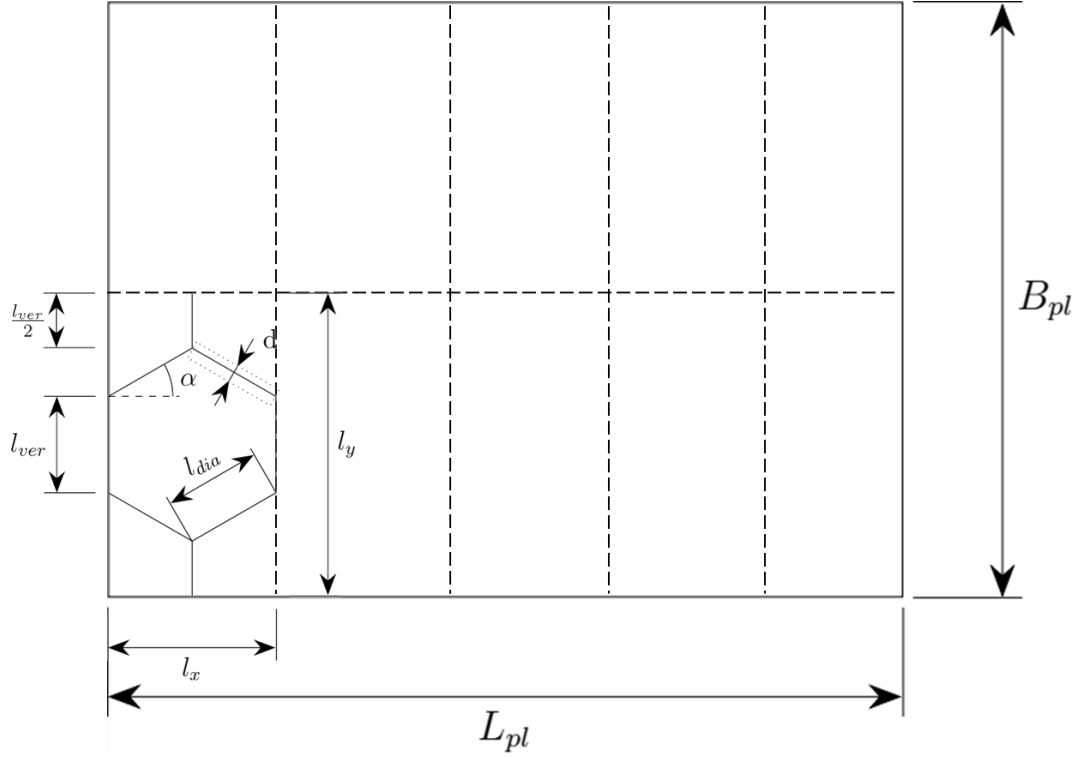$$l_y = \frac{B_{PL}}{n_v} \tag{2}$$

Fig. 2 – Plane for the honeycomb core with overall dimensions, an arbitrary division of the honeycomb cells and one cell with dimensions similar to literature[3,4].

The diagonal length l_{dia} and the vertical length l_{ver} are not the same because the cell angle is one of the variables. In case of a variable cell angle the diagonal and vertical length are calculated with:

$$l_{dia} = \frac{l_x}{2 * \cos(\alpha)} = \frac{L_{PL} - d}{2 * n_h * \cos(\alpha)} \tag{3}$$

$$l_{ver} = \frac{l_y}{2} - \sin(\alpha) * l_{dia} \tag{4}$$

The next step is the calculation of the volume from a single cell. It has to be noticed that adjacent cells in horizontal direction share the vertical wall on the left and on the right side. Therefore, the volume of a cell is calculated without the right vertical wall. It is assumed that the right wall is already part of the adjacent cell.

$$V_{cell} = (2 * l_{ver} + 4 * l_{dia}) * d * H_{PL} \tag{5}$$

Now, the overall volume of the honeycomb core can be calculated. The number of the cells is given and can be multiplied with the cell volume from equation (5). The cells on the far right, which have no neighboring cell on their right, do not have a vertical wall. This disregard has to be added to the overall volume.

$$V_{over} = n_v * n_h * V_{cell} + n_v * l_{ver} * d * H_{PL} - d^2 * K \tag{6}$$

In equation (6) a correction factor K is added. This is necessary, because the lines of the cells are extruded as a rectangle. If these lines are crossing, then overlapping areas arise like in figure 3. The top overlapping area has a different surface area than the other two. The surface areas are formulated as:

$$A_{sq1} = \frac{d^2}{4} * \tan\left(\frac{90° - \alpha}{2}\right) \tag{7}$$

$$A_{sq2} = \frac{d^2}{4} * \tan(\alpha) \tag{8}$$

The overlapping areas arise for each crossing of three lines. The equation for the correction is then:

$$d^2 * K = \left(2 * A_{sq1} + A_{sq2}\right) * \left(2 * n_h * n_v + 2 * (n_h - 1) * n_v\right) * H_{PL} \tag{9}$$
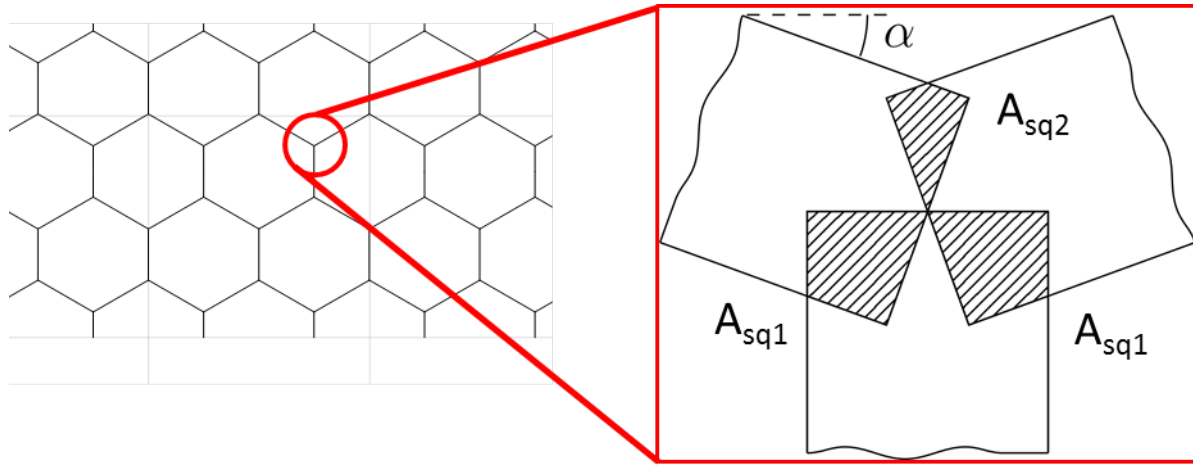

Fig. 3 – Overlapping areas of honeycomb core when the cell walls are extruded.

Now, the equations (1) – (5) and (7) – (9) are inserted into equation (6). Then, a formulation is available to calculate the thickness of the cell in dependency of the 8 parameters. The height H_{PL} is present in all terms and is divided through the volume.

$$
\begin{aligned}
\frac{V_{over}}{H_{PL}} = d &\left[B_{PL} * n_h + L_{PL} * n_v * \frac{2 - \sin(\alpha)}{\cos(\alpha)} + \frac{B_{PL}}{2} - \tan(\alpha) \right. \\
&\left. * \frac{L_{PL} * n_v}{2 * n_h} \right] \\
+ d^2 &\left[-n_v * \frac{2 - \sin(\alpha)}{\cos(\alpha)} + \tan(\alpha) * \frac{n_v}{2 * n_h} - n_v \right. \\
&\left. * (2 * n_h - 1) * \left(\tan\left(\frac{90° - \alpha}{2}\right) + \frac{tan(\alpha)}{2}\right) \right]
\end{aligned}
\tag{10}
$$

$$\frac{m_{tar}}{H_{PL} * \rho_{core}} = V_{lin} * d + V_{quad} * d^2 \tag{11}$$

In contrast to literature[3,4], the formulation of the thickness is a quadratic problem in equation (10). In equation (11) the volume from equation (10) is replaced by mass and density and two factors are introduced, which summarize the square brackets in equation (10). Two zeros exist for equation (11), which are both positive. The zero with the smaller value is the solution for the honeycomb core. The zero with the higher value generates a solid core instead of a honeycomb core.

2.2 Finite element model

After the core architecture has been calculated in the x-y plane, it is extruded as volume with the CAD software CATIA[TM]. Also, the face sheets are added as volume in the model with a thickness of one Millimeter. One example of the overall core geometry is shown in figure 4. The complete volume is the baseline for the finite element analysis in ANSYS®. The generated model does not regard any adhesive between face sheet and the core because the volume is meshed as a single volume. The result is a mesh, which is irregular. The elements are tetrahedral with a quadratic formulation. Therefore, the expected structural behavior in the simulation will probably be stiffer than in the future experiments.
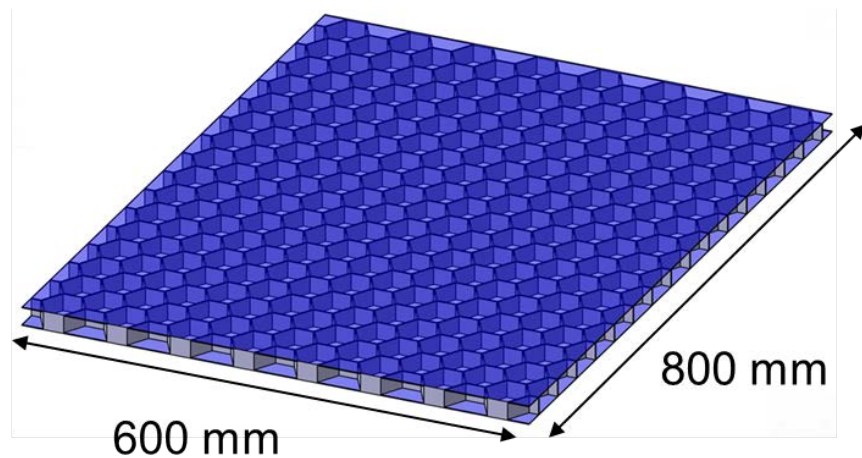

Fig. 4 – CAD model of 3D sandwich core with face sheets.

The manufacturing of the core will be realized with an additive layer manufacturing process. The material of the core is the SL-Tool® NewWhite from the company Robotmech. The face sheets will be the FR4 epoxy resin glass laminated fabric with a thickness of one Millimeter. The name of the fabric is EP GC 202 comparable to DIN EN 60893. For both materials datasheets exist, which are the baseline of the material properties in the simulation[5,6]. The material models are both linear and isotropic. Table 1 summarizes the general material data, which is used in ANSYS® Workbench[TM].

Table 1 – Material parameters for the linear isotropic material models in the simulation[5,6].

Material	Density [kg/m³]	Young's modulus [N/m²]	Poisson ratio [-]
EP GC 202	1800	18 e9	0.26
SL-Tool NewWhite	1230	2.6 e9	0.3

2.3 Excitation Generation

The main objective of the excitation is the calculation of nodal forces which can be applied to the nodes of one face sheet. The baseline is a hemisphere where the structure is in the middle of the circle and the monopole sources are arranged at the hemisphere. Figure 5 shows an example with a rectangular plate and a hemisphere with a unit radius. In order to achieve far field condition the radius is set to 100 meters. It is possible to vary the number of sources at the hemisphere. If the number is set to one monopole source the position of this source is at the zenith and the excitation is equal to a plane wave.
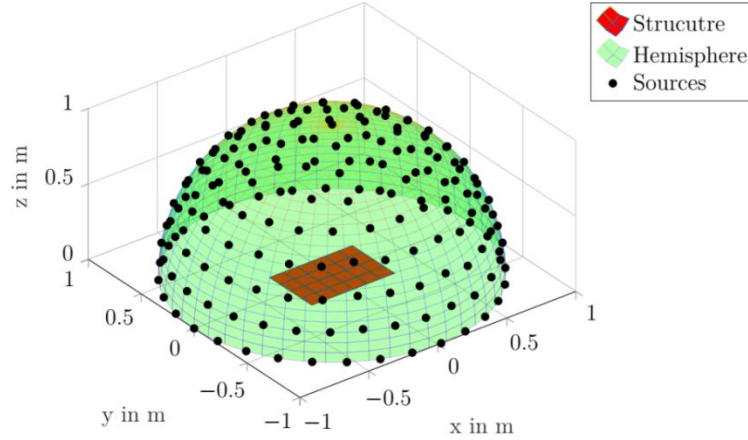

Fig. 5 – Hemisphere with unit radius, monopole source positions and arbitrary plate in the middle of the circle.

Each monopole source radiates a sound wave to the mesh points of the structure. For a single source and a single mesh point the pressure at the mesh point can be calculated[7,8]. Figure 6 shows the relation between the monopole source Q_P and the structural point S_P.
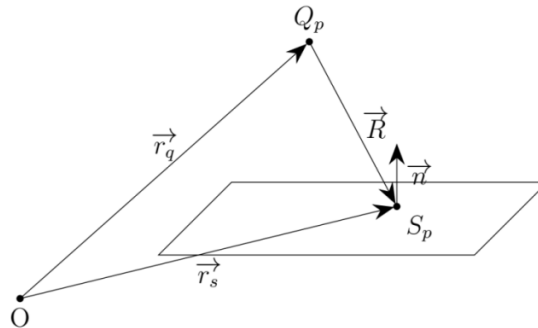

Fig. 6 – Relation between the monopole source and the structural point.

The pressure at the surface of the point S_P is defined as[7,8]:

$$p = \frac{j * \rho_0 * \omega * q}{4 * \pi * |\vec{R}|} * e^{-j*k*|\vec{R}|+\varphi} \tag{12}$$

Where j is the imaginary unit, ρ_0 is the density of air, ω is the natural frequency, q is the volume flow of the medium, $\vec{R}$ is the vector between source and structural point, k is the wave number and φ is an arbitrary angle. The arbitrary angle is a phase shift and it is relevant for the

superposition of the pressure for each source point at one structural point. For each structural point a pressure is calculated as a superposition from each source on the hemisphere with equation (12).

For the irregular mesh of the face sheet an area for each mesh point must be calculated to get an equivalent nodal force instead of the pressure. Figure 7 shows the relevant area with green shading for the red circled mesh point. The mesh of the face sheet surface is triangular. The shaded area consists of one third of each triangular element where the red mesh point is part of the element. The medians (M) of two edges and the barycenter (BC) are required to get the third of one element. The connection of all medians and barycenters is the polygon in figure 7, which is the related area for the red circled mesh point. The overall area is than multiplied with the calculated pressure from equation (12) for each source to get the nodal force at this point.
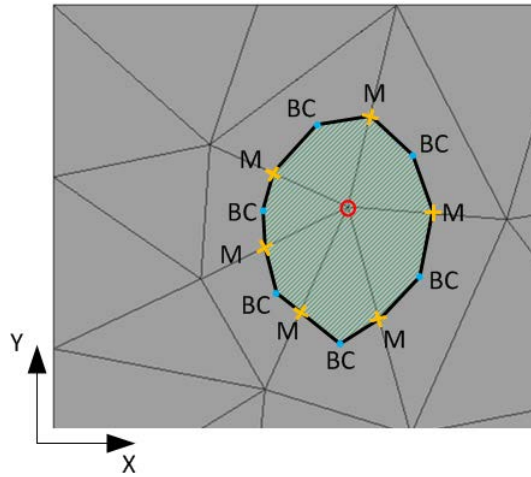

Fig. 7 – Part of a face sheet mesh with the regarded mesh point (red circled), the barycenters (BC) of related triangles, the medians (M) of the related edges and the shaded area for the calculation of the equivalent nodal force.

2.4 Transmission loss calculation

The TL is the ratio of the incident intensity to the radiated intensity[7]. In this work the ratio of the sound power is used, because the face sheets are equivalent in their area.

$$TL = 10 * \log_{10}\left(\frac{P_{in}}{P_{rad}}\right) \tag{13}$$

The calculation of the incident sound power is based on the pressure distribution on the face sheet. This distribution is already calculated with equation (12) for each structural point. The incident sound power on the face sheet surface is given with the mean pressure of the diffuse field p_{mean} [9].

$$P_{in} = \frac{p_{mean}^2 * S}{4 * \rho_0 * c_0} \tag{14}$$

In equation (14) S is the surface area of the face sheet, ρ_0 is the density of air and c_0 is the speed of sound in air. The equation (14) is valid, if far field conditions are present. In case of the hemisphere radius the far field condition is already fulfilled. The incident angle ϑ of the diffuse

field varies between 0° and 90°. Therefore, the cosines of the incident angle are set to 0.5 in equation (14). The excitation generator is able to generate a plane wave excitation with one source at the hemisphere. The incident angle of the plane wave is 0° and the cosine is 1. In case of an incident wave from the hemisphere equation (14) has to be multiplied with 2 to get the incident sound power.

For the radiated sound power of the sandwich panel the velocity of the radiating face sheet is necessary. The sound power of a plate is calculated with the radiation resistance matrix Z and the structural velocity vector $\vec{v}$ [10].

$$P_{rad} = \vec{v}^H * Z * \vec{v} \qquad (15)$$

In order to calculate the radiation resistance matrix the surface of the face sheet is divided in a regular grid with rectangular elements. The rectangular elements are similar to an elementary radiator with the area A. At the node of these elements the velocity is interpolated from the results of the irregular finite element mesh. The radiation matrix is calculated equal to the literature[10].

$$Z = \frac{\omega^2 * \rho_0 * A^2}{4 * \pi * c_0} * \begin{bmatrix} 1 & \frac{\sin(k*r_{12})}{k*r_{12}} & \cdots & \frac{\sin(k*r_{1n})}{k*r_{1n}} \\ \frac{\sin(k*r_{21})}{k*r_{21}} & 1 & \cdots & \vdots \\ \vdots & \vdots & \ddots & \vdots \\ \frac{\sin(k*r_{n1})}{k*r_{n1}} & \cdots & \cdots & 1 \end{bmatrix} \qquad (16)$$

In the matrix Z is r_{ij} the distance between the single elementary radiators. It is obvious that the distance r_{ij} is equal to r_{ji} and thus the matrix is quadratic and symmetric with the size of the node numbers n.

3   SIMULATION RESULTS

In order to achieve equivalent excitations for different sandwich configurations there are two options. The first one is to sum the TL for different diffuse excitation for one sandwich plate. The second possibility is to use a plane wave excitation with only one source at the zenith of the hemisphere. The presented results are simulated with the plane wave excitation. Also, the results are limited to the two parameters cell angle α and the vertical number of cells n_h.

In the calculation of the structural response a constant structural damping coefficient is used. For that damping type in ANSYS® the damping force is proportional to the displacement. The coefficient depicts only internal material friction and is set to 0.04. Hence, eigenmodes can be identified as drops in the TL.

3.1 Results of the vertical number variation of the honeycomb core

Figure 8 shows three different honeycomb cores where the number of vertical cells is 4, 8 and 16. The different numbers result in a different vertical length l_{ver} and a different thickness of the core. The horizontal number of cell is 16 and the cell angle is 30°.
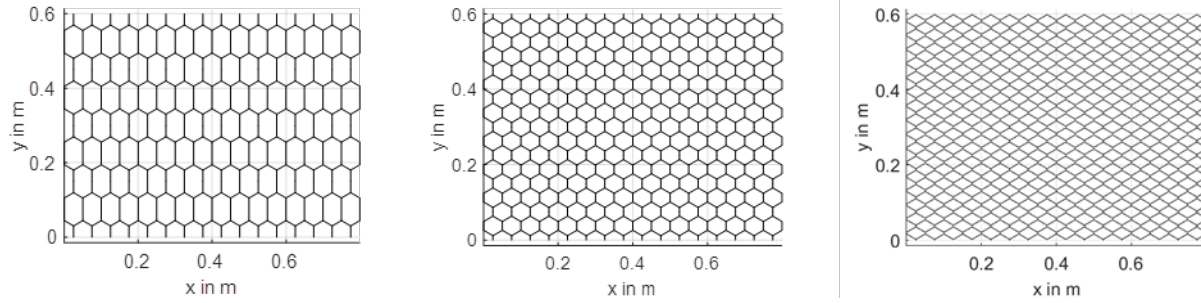
Fig. 8 – Core geometries with 4 (left), 8(middle) and 16(right) cells in vertical direction.

Figure 9 shows the curves of the plane wave TL for the three configurations from figure 8. The regarded frequency range reaches from 100 Hz to 1000 Hz and is presented in logarithmic scale. The drops in figure 9 indicate eigenmodes of the structure which are excited by the plane wave.

The variation of the cell numbers shows an influence on the TL. Mainly, the frequency bandwidth between the natural frequencies varies. There is no general tendency that a higher cell number increase the natural frequency of all eigenmodes. Also, the first natural frequency is not influenced by the variation. The curve progression is up to approximately 400 Hz nearly equal. Afterwards, the amplitude of the TL and the natural frequency of eigenmodes are changing.
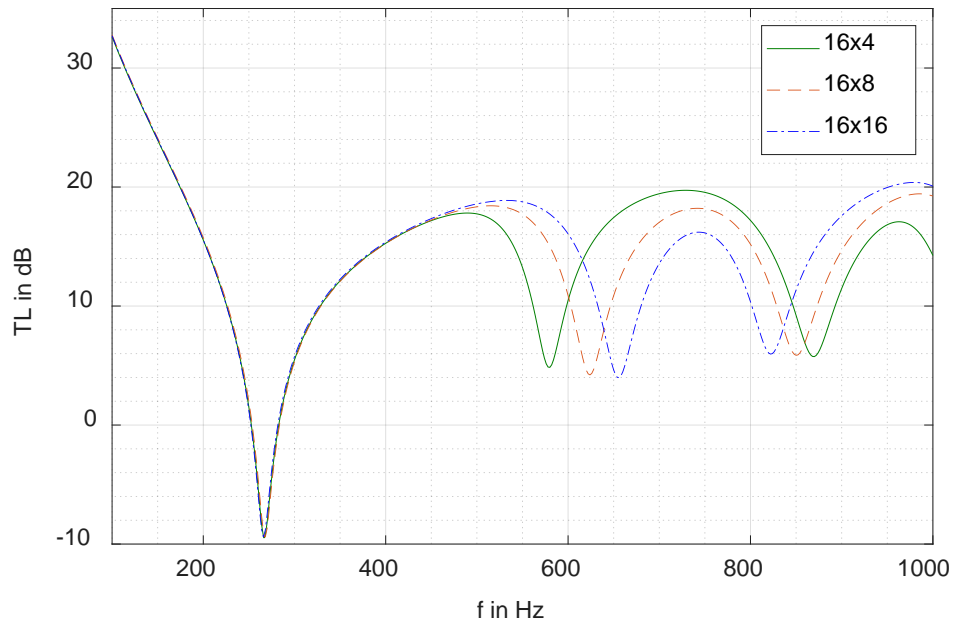

Fig. 9 – Transmission loss of the vertical cell number variation.

3.2 Results of the angle variation of the honeycomb core

The second part of the results shows the influence of the cell angle variation. Figure 10 shows the honeycomb core for three different angles with -30°, 30° and 45°. The number of cells in horizontal direction is 16 and in vertical direction 8. Due to the angle variation the sum of all cell lengths is different. This results in different thicknesses for each configuration.
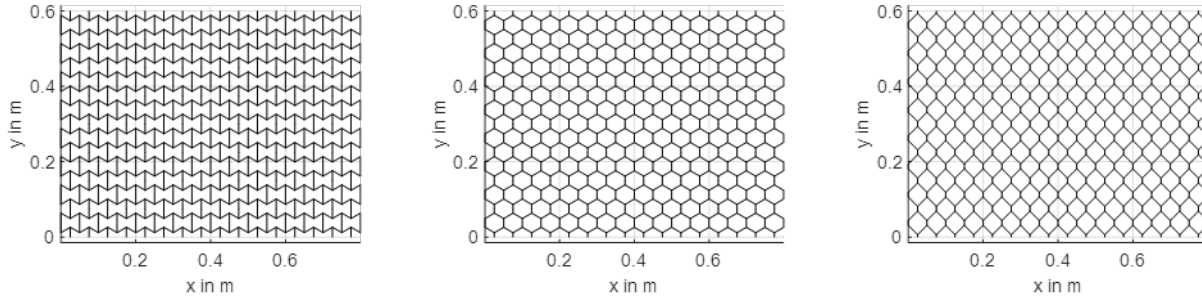
Fig. 10 – Core geometries with -30° (left), 30° (middle) and 45° (right) angle of the cell.

The influence of the angle variation in the TL is shown in figure 11. The difference on the TL is less significant compared to the variation of the vertical cell numbers. The shift of the natural frequency starts at 700 Hz in figure 11. The change on the TL is a result of the different thicknesses of the cores. The overall length of the core geometry in figure 10 varies for each configuration and that leads to different thicknesses.
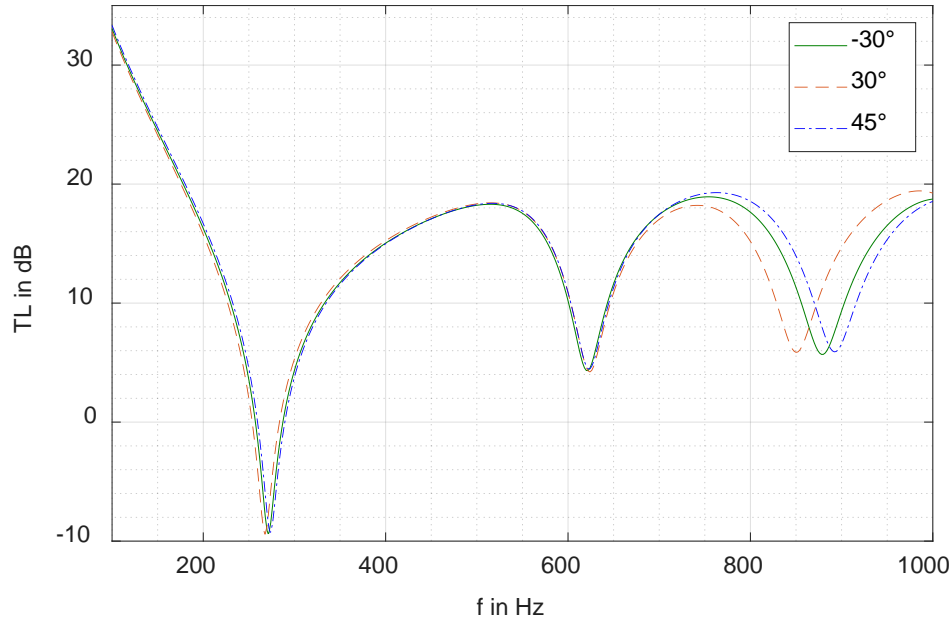

Fig. 11 – Transmission loss of the cell angle variation.

4   CONCLUSIONS

The variation of geometrical parameters influences the transmission loss (TL) at the frequency range from 100 Hz up to 1000 Hz where the eigenmodes have a major influence. The presented framework models different honeycomb cores, which are defined by 8 parameters. The mass between these configurations has been kept constant in order to exclude the influence of additional mass. After the honeycomb design the framework calculates a plane wave excitation with equivalent nodal force on the face sheet of the sandwich. With a finite element analysis the structural response is determined. The incident sound power and the radiated sound power are calculated without fluid elements in order to reduce the computational costs. The TL is the ratio of these two sound power values. The results show that the variation of honeycomb core properties like core angle or number of cells in vertical direction influence the TL. The natural

frequencies except the first one are shifted in the regarded frequency range. Also, the amplitude of the TL changes with the core variation. The influence on the TL starts at approximately 400 Hz.

The framework is the baseline for following sensitivity analysis in order to analyze the behavior of each parameter. Some configurations are planned to be produced with an additive layer manufacturing process and will be analyzed in an acoustic test rig in order to validate the results from the simulation.

5   REFERENCES

1. Jae-Deok Jung and Suk-Yoon Hong and Jee-Hun Song and Hyun-Woung Kwon, "A Study on Transmission Loss Characteristics of Honeycomb Panel for Offshore Structures", *Journal of Applied Mathematics and Physics*, **03**(2), 172 – 176, (2015).

2. Sathish Kumar, *Sound transmission properties of honeycomb panels and double-walled structures*, PhD, KTH The Royal Institute of Technology, Stockholm, Sweden, (2012).

3. Rohan Galgalikar and Lonny L. Thompson, "Design Optimization of Honeycomb Core Sandwich Panels for Maximum Sound Transmission Loss", J*ournal of Vibration and Acoustics,* **138**(5), 051005-1 – 051005-13, (2016).

4. David Griese and Joshua D. Summers and Lonny Thompson, "Experimental study of noise reduction in centrifugal blowers", *Journal of Vibration and Acoustics,* **137**(2), 021011-1 – 021011-11, (2015).

5. ZUK, *Werkstoffdaten Glashartgewebe*, Z+K Stanzteile GmbH, Lohmühlenweg 18, 99326 Stadtilm, Germany, See also URL: http://www.zuk-stanzteile.de/download /glashartgewebe.pdf (Last accessed: 26.04.18).

6. Robotmech*: SL-Tool® NewWhite datasheet*, Robotmech Stössl GmbH, Bundesstraße 11, 6842 Koblach, Austria, See also URL: https://www.robotmech.com/fileadmin/media/ downloads/Datasheets/Stereolithografie/robotmech-SL-TOOL-NewWhite.pdf (Last accessed: 26.04.18).

7. Frank Fahy and Paolo Gardonio, *Sound and structural vibration: Radiation, transmission and response,* 2. ed., Elsevier (Academic Press), Oxford, (2008).

8. Stephan Tewes, *Active Trim Panel Attachments for Control of Sound Transmission through Aircraft Structures*, PhD, Technical University Munich, Germany, (2006).

9. Michael Möser, *Technische Akustik,* 6. ed., Springer, Berlin, Heidelberg, (2005).

10. Stephen J. Elliott and Marty E. Johnson, "Radiation modes and the active control of sound power", *The Journal of the Acoustical Society of America*, **94** (4), 2194 – 2204, (1993).